

A structural approach to relaxation in glassy liquids

S. S. Schoenholz^{1*}†, E. D. Cubuk^{2†}, D. M. Sussman¹, E. Kaxiras² and A. J. Liu^{1*}

In contrast with crystallization, there is no noticeable structural change at the glass transition. Characteristic features of glassy dynamics that appear below an onset temperature, T_0 (refs 1–3), are qualitatively captured by mean field theory^{4–6}, which assumes uniform local structure. Studies of more realistic systems have found only weak correlations between structure and dynamics^{7–11}. This raises the question: is structure important to glassy dynamics in three dimensions? We answer this question affirmatively, using machine learning to identify a new field, ‘softness’ which characterizes local structure and is strongly correlated with dynamics. We find that the onset of glassy dynamics at T_0 corresponds to the onset of correlations between softness (that is, structure) and dynamics. Moreover, we construct a simple model of relaxation that agrees well with our simulation results, showing that a theory of the evolution of softness in time would constitute a theory of glassy dynamics.

To look for correlations between structure and dynamics, one typically tries to find a quantity that encapsulates the important physics, such as free volume, bond orientational order, locally preferred structure, and so on. In contrast to this approach, we use a machine learning method designed to find a structural quantity that is strongly correlated with dynamics. Earlier, we applied this approach to the simpler problem of classifying particles as being ‘soft’ if they are likely to rearrange or ‘hard’ otherwise¹². We describe a particle’s local structural environment with $M = 166$ ‘structure functions’¹³ that respect the overall isotropic symmetry of the system and include radial density and bond angle information. We then define an M -dimensional space, \mathbb{R}^M , with an orthogonal axis for each structure function. The local structural environment of a particle i is thus encoded as a point in M -dimensional space. We assemble a ‘training set’ from molecular dynamics simulations consisting of equal numbers of ‘soft’ particles that are about to rearrange and ‘hard’ particles that have not rearranged in a time τ_α preceding their structural characterization, and find the best hyperplane separating the two groups using the support vector machines (SVM) method^{14,15}. Finally, we define the softness, S_i , of particle i as the shortest distance between its position in \mathbb{R}^M and the hyperplane, where $S_i > 0$ if i lies on the soft side of the hyperplane and $S_i < 0$ otherwise.

We study a 10,000-particle 80:20 bidisperse Kob–Andersen Lennard-Jones glass¹⁶ in three dimensions at different densities ρ and temperatures T above its dynamical glass transition temperature. All results here are for particles of species A only. However, the results are qualitatively the same for particles of both species. At each density we select a training set of 6,000 particles, taken from a molecular dynamics trajectory at the lowest T studied,

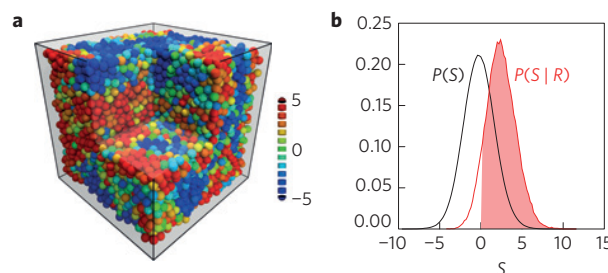


Figure 1 | The characteristics of the softness field. **a**, A snapshot of the system at $T = 0.47$ and $\rho = 1.20$ with particles coloured according to their softness from red (soft) to blue (hard). **b**, The distribution of softness of all particles in the system (black) and of those particles that are about to rearrange (red). 90% of the particles that are about to rearrange have $S > 0$ (shaded region). None of the data included in this plot were in the training set.

to construct a hyperplane in \mathbb{R}^M . We then use this hyperplane to calculate $S_i(t)$ for each particle i at each time t during an interval of $30,000\tau$ at each ρ and T .

We can deduce the most important structural features contributing to softness either by training on fewer structure functions or by examining the projection of the hyperplane normal onto each orthogonal structure function axis. Both analyses yield a consistent picture (see Supplementary Information): the most important features are the density of neighbours at the first peaks of the radial distribution functions $g_{AA}(r)$ and $g_{AB}(r)$; these two features alone give 77% prediction accuracy for rearrangements. Particles with more neighbours at the first peaks of $g(r)$ have a lower softness, and are thus more stable. These results are reminiscent of the cage picture, in which an increase of population in the first-neighbour shell suppresses rearrangements, or the free-volume picture, in which particles whose surroundings are closely packed are more stable than those with more loosely packed neighbourhoods¹⁷. Overall, soft particles typically have a structure that is more similar to a higher-temperature liquid, where there are more rearrangements, whereas hard particles have a structure that is closer to a lower-temperature liquid¹⁸.

Figure 1a is a snapshot with particles coloured according to their softness. Evidently, S has strong spatial correlations. Figure 1b shows the distribution of softness, $P(S)$, and the distribution of softness for particles just before they go through a rearrangement, $P(S|R)$. We see that 90% of the particles that undergo rearrangements have $S > 0$. We have also tested other sets of structure functions (see Supplementary Information) and found nearly identical accuracy. Softness is therefore a highly accurate predictor of

¹Department of Physics and Astronomy, University of Pennsylvania, 209 South 33rd Street, Philadelphia, Pennsylvania 19104, USA. ²Department of Physics and School of Engineering and Applied Sciences, Harvard University, Cambridge, Massachusetts 02138, USA. [†]These authors contributed equally to this work. *e-mail: schsam@sas.upenn.edu; ajliu@sas.upenn.edu

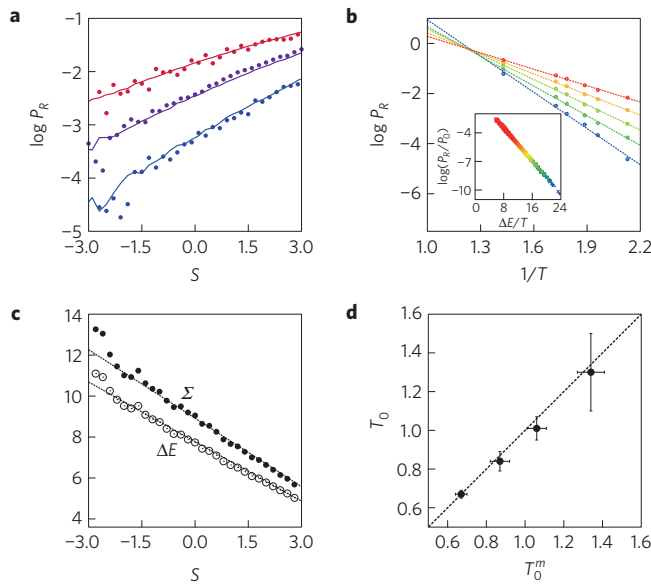


Figure 2 | The relationship between softness and dynamics. **a**, The probability that particles rearrange as a function of their softness, $P_R(S)$, for temperatures $T=0.47, 0.53$ and 0.58 plotted in blue, purple and red, respectively. Solid lines are measurements from molecular dynamics trajectories. Points represent the probabilities calculated from the zero-time derivative of the overlap, $-dq(S, t)/dt$. **b**, $P_R(S)$ as a function of $1/T$ for five different softness values from $S \sim -3$ (blue) to $S \sim 3$ (red). The inset shows the collapse of these probabilities when P_R/S_0 is plotted against $\Delta E/T$. **c**, ΔE and Σ , where $P_R(S) = \exp(\Sigma - \Delta E/T)$, versus softness S . **d**, Predicted onset temperature T_0 versus T_0^m , the onset temperature measured by Keys, *et al.*²⁰, for densities $\rho=1.15, 1.20, 1.25, 1.30$. The straight line corresponds to $T_0 = T_0^m$.

rearrangements that is reasonably robust to the set of structure functions chosen.

We next show that the probability that particles rearrange is a function of their softness. This probability is calculated as the fraction of particles of a softness, S , that are rearranging at a given time, $P_R(S)$. We plot $P_R(S)$ in Fig. 2a in solid lines at temperatures ranging from $T=0.47$ (blue) to $T=0.58$ (red). At each T we see that $P_R(S)$ is a strong function of softness, increasing by several orders of magnitude, especially at the lower temperatures, in the range $S=-3$ to $S=3$. A similar, albeit more modest, relationship was seen in ref. 19. When $P_R(S)$ is plotted as a function of $1/T$ for several values of softness (Fig. 2b), the probability that a particle of softness S will rearrange has Arrhenius behaviour, $P_R(S) = P_0(S) \exp(-\Delta E(S)/T)$, where $P_0(S)$ and $\Delta E(S)$ depend on S . Confirming this observation, $P_R(S)/P_0(S)$ collapses over many orders of magnitude for all temperatures when plotted against $\Delta E(S)/T$, as shown in the inset of Fig. 2b.

An Arrhenius form emerges when a kinetic process depends on a single energy scale $\Delta E(S)$. In Fig. 2c we plot $\Delta E(S)$ and $\Sigma(S) \equiv \ln P_0(S)$ versus S . Both terms depend nearly linearly on S : $\Delta E = e_0 - e_1 S$ and $\Sigma = \Sigma_0 - \Sigma_1 S$, where all four coefficients are positive and independent of T . Our results are consistent with the interpretation that, at low temperatures, harder regions of the glassy liquid with higher energy barriers are frozen out whereas softer regions are not, leading to heterogeneous dynamics. These heterogeneities smooth out with increasing temperature, and vanish altogether once $P_R(S)$ no longer depends on softness. This occurs at the temperature T_0 where the softness dependence of Σ exactly cancels that of $\Delta E/T_0$, and so $T_0 = e_1/\Sigma_1$. This result can also be seen visually in Fig. 2b, where the different Arrhenius predictions for $P_R(S)$ all intersect at a single temperature, T_0 , where the probability of rearrangement will be independent of softness. In

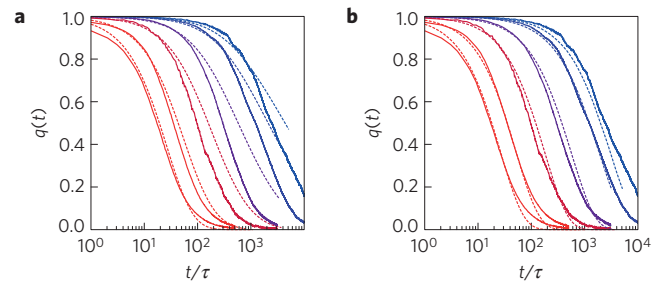


Figure 3 | Overlap calculated from softness. **a**, Solid lines are the measured overlap function, for temperatures $T=0.45, 0.47, 0.53, 0.58, 0.63$ and 0.70 , from blue to red, respectively. The dashed lines show predictions assuming each Arrhenius process is independent of one another. **b**, The solid lines are the same as in **a**. Dashed lines are predictions for the overlap function from $P_R(S)$ including changes in the softness field induced by spatial correlation between rearranging particles.

Fig. 2d we compare our prediction for T_0 to the onset temperature of glassy dynamics measured by Keys *et al.*²⁰, T_0^m , at different densities. The excellent agreement between the predicted T_0 and the measured values implies that the onset of glassy dynamics at $T=T_0$ coincides with the onset of correlations between structure (softness) and dynamics.

We explore next the relationship between softness and the non-exponential decay of the overlap function

$$q(t) = \frac{1}{N} \sum_i \Theta(a - |r_i(t) - r_i(0)|)$$

where N is the number of particles in the system, r_i is the position of particle i , and Θ is the Heaviside function. We take $a=0.5$ (ref. 21). In Fig. 3a,b we plot the overlap function for different temperatures at $\rho=1.20$. Our aim is to understand the form of the decay of $q(t)$ from the behaviour of the rearrangement probability, $P_R(S)$. To begin, we define the contribution to the overlap from particles whose softness was initially S at $t=0$, $q(S, t)$. The total overlap is $q(t) = \int dS q(S, t) P(S)$. Because $q(S, t)$ is the fraction of particles with initial softness S that have not rearranged after a time t , we expect $(dq(S, t)/dt)|_{t=0} = -c_a P_R(S)$ (see Supplementary Information for details), where c_a is the fraction of rearrangements that displace particles by more than a . This is indeed the case, as is evident from the data in Fig. 2a, when $(dq(S, t)/dt)|_{t=0}$ (points) is overlaid with $P_R(S)$ (solid lines).

If we now assume that each particle rearranges with probability $P_R(S)$ as an independent Arrhenius process according to Fig. 2, then we can predict the decay of $q(S, t)$ using a simple discrete model: it can be written in terms of the probability that a particle of softness S does not rearrange for $t-1$ time steps before finally rearranging at time t , given by $(1 - P_R(S))^{t-1} P_R(S)$. The resulting prediction for $q(t)$ (dashed) is shown in Fig. 3a for several different temperatures. Although the prediction is not poor, its accuracy decreases at longer times, particularly at lower temperatures.

We now show that the discrepancy between our naive theory and the decay of $q(t)$ primarily results from a crucial neglected feature: even if a given particle does not rearrange, its local structural environment—and therefore its softness—can be altered if nearby particles rearrange. This physics is reminiscent of facilitation.

To take this facilitation into account, we calculate the ‘softness propagator’, $G(S, S_0, t)$, defined as the distribution of softness at time t for particles that start with a softness S_0 at $t=0$ and move less than a distance a after a time t (that is, that do not rearrange in a time t). Figure 4a shows a Gaussian approximation to $G(S, S_0, t)$. We see that $G(S, S_0, t)$ is sharply peaked around S_0 at small t , but widens and shifts with increasing t , reminiscent of

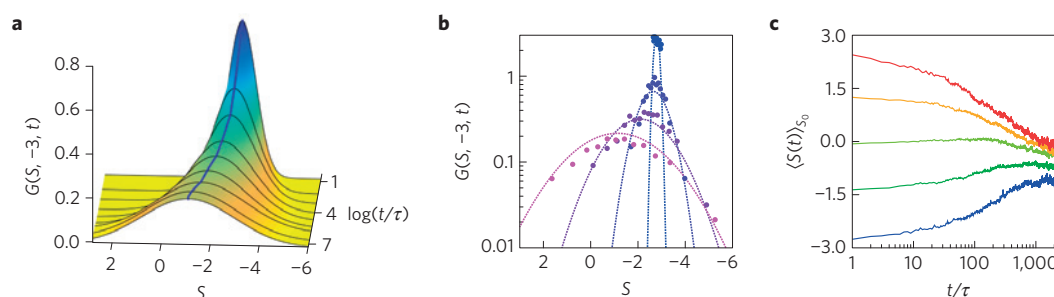


Figure 4 | Time evolution of softness. **a**, The stochastic evolution of softness in time as seen through the evolution of the Gaussian approximation to the distribution of softness. **b**, The time evolution of the softness distribution for a collection of particles with initial softness $S_0 \sim -3$ from $t=0$ (blue) to $t=1,000\tau$ (pink). Points are the measured histogram values, and the dashed lines are Gaussian approximations to the distribution. **c**, The time evolution of the average softness for particles that start from several softness values ranging from $S_0 \sim -3$ (blue) to $S_0 \sim 3$ (red).

directed diffusion. Figure 4b shows $G(S, S_0 = -3, t)$ at several different times, where points are measured probabilities and dashed lines are their Gaussian approximations. In Fig. 4c we plot the mean softness evaluated as $\langle S(t) \rangle_{S_0} = \int dS S G(S, S_0, t)$ for several different values of S_0 . For each S_0 the average softness of particles evolves towards the mean of the equilibrium softness distribution over a time period of approximately τ_a . The softness propagator is evaluated only for particles that have not rearranged, so Fig. 4 shows that rearrangements of nearby particles affect a particle's softness significantly.

Our first naive prediction based on the assumption that particles rearrange independently corresponds to $G(S, S_0, t) = \delta(S - S_0)$. We refine our theory by using the actual softness propagator in connecting the probability of rearranging, $P_R(S)$, with the overlap $q(S, t)$ (see Supplementary Information). For ease of calculation, we approximate $G(S, S_0, t)$ as a Gaussian distribution in S and calculate its mean and variance as functions of S_0 and t from simulated data. The resulting prediction for the overlap is shown in Fig. 3b. The agreement with the actual $q(t)$ is excellent, suggesting that an understanding of the time evolution of the softness field, or equivalently of the softness propagator, would suffice to understand the non-exponential decay of the overlap function.

Our results show that there is structure hidden in the disorder of glassy liquids. This structure can be quantified by softness, which controls glassy dynamics at temperatures below T_0 . According to our analysis, simple Arrhenius relaxation for each softness, coupled with the time evolution of softness, leads to the observed slow, non-exponential relaxation dynamics of glassy liquids below T_0 . Thus, our results suggest that the challenge of understanding glass transition dynamics can be reframed as the challenge of understanding the evolution of softness.

Methods

Methods and any associated references are available in the [online version of the paper](#).

Received 24 June 2015; accepted 18 December 2015;
published online 1 February 2016

References

1. Angell, C. A. Formation of glasses from liquids and biopolymers. *Science* **267**, 1924–1935 (1995).
2. Sastry, S., Debenedetti, P. G. & Stillinger, F. H. Signatures of distinct dynamical regimes in the energy landscape of a glass-forming liquid. *Nature* **393**, 554–557 (1998).
3. Debenedetti, P. G. & Stillinger, F. H. Supercooled liquids and the glass transition. *Nature* **410**, 259–267 (2001).
4. Parisi, G. & Zamponi, F. Mean-field theory of hard sphere glasses and jamming. *Rev. Mod. Phys.* **82**, 789 (2010).
5. Berthier, L., Biroli, G., Bouchaud, J.-P., Cipelletti, L. & van Saarloos, W. *Dynamical Heterogeneities in Glasses, Colloids, and Granular Media* (Oxford Scholarships Online, 2011).

6. Charbonneau, P., Kurchan, J., Parisi, G., Urbani, P. & Zamponi, F. Exact theory of dense amorphous hard spheres in high dimensions. III. the full RSB solution. *J. Stat. Mech.* P10009 (2014).
7. Gilman, J. Metallic glasses. *Phys. Today* **28**, 46–53 (May, 1975).
8. Berthier, L. & Jack, R. L. Structure and dynamics of glass formers: predictability at large length scales. *Phys. Rev. E* **76**, 041509 (2007).
9. Royall, C. P., Williams, S. R., Ohtsuka, T. & Tanaka, H. Direct observation of a local structural mechanism for dynamic arrest. *Nature Mater.* **7**, 556–561 (2008).
10. Manning, M. L. & Liu, A. J. Vibrational modes identify soft spots in a sheared disordered packing. *Phys. Rev. Lett.* **107**, 108302 (2011).
11. Jack, R. L., Dunleavy, A. J. & Royall, C. P. Information-theoretic measurements of coupling between structure and dynamics in glass-formers. *Phys. Rev. Lett.* **113**, 095703 (2014).
12. Cubuk, E. D. et al. Identifying structural flow defects in disordered solids using machine learning methods. *Phys. Rev. Lett.* **114**, 108001 (2015).
13. Behler, J. & Parrinello, M. Generalized neural-network representation of high-dimensional potential-energy surfaces. *Phys. Rev. Lett.* **98**, 146401 (2007).
14. Chang, C.-C. & Lin, C.-J. LIBSVM: a library for support vector machines. *ACM Trans. Intell. Syst. Technol.* **2**, 27 (2011).
15. Cortes, C. & Vapnik, V. Support-vector networks. *Mach. Learn.* **20**, 273–297 (1995).
16. Kob, W. & Andersen, H. C. Scaling behavior in the β -relaxation regime of a supercooled Lennard-Jones mixture. *Phys. Rev. Lett.* **73**, 1376 (1994).
17. Berthier, L. & Biroli, G. Theoretical perspective on the glass transition and amorphous materials. *Rev. Mod. Phys.* **83**, 587–645 (2011).
18. Percus, J. K. & Yevick, G. J. Analysis of classical statistical mechanics by means of collective coordinates. *Phys. Rev.* **110**, 1–13 (1958).
19. Smessaert, A. & Rottler, J. Structural relaxation in glassy polymers predicted by soft modes: a quantitative analysis. *Soft Matter* **10**, 8533–8541 (2014).
20. Keys, A. S., Hedges, L. O., Garrahan, J. P., Glotzer, S. C. & Chandler, D. Excitations are localized and relaxation is hierarchical in glass-forming liquids. *Phys. Rev. X* **1**, 021013 (2011).
21. Keys, A. S., Abate, A. R., Glotzer, S. C. & Durian, D. J. Measurement of growing dynamical length scales and prediction of the jamming transition in a granular material. *Nature Phys.* **3**, 260–264 (2007).

Acknowledgements

We thank D. Chandler, K. Mandadapu, M. Parrinello, J. Sethna and D. Wales for helpful discussions. This work was supported by the US Department of Energy, Office of Basic Energy Sciences, Division of Materials Sciences and Engineering under Award DE-FG02-05ER46199 (S.S.S. and A.J.L.), the Advanced Materials Fellowship of the American Philosophical Society (D.M.S.), a Harvard IACS Student Scholarship (E.D.C.), and a Simons Investigator award from the Simons Foundation (A.J.L.).

Author contributions

E.D.C. and S.S.S. contributed equally to this work. S.S.S. and E.D.C. conceived the project, did the simulations, and analysed the data. A.J.L. supervised the project and analysis. All authors contributed to analysis, discussion and writing of the manuscript.

Additional information

Supplementary information is available in the [online version of the paper](#). Reprints and permissions information is available online at www.nature.com/reprints. Correspondence and requests for materials should be addressed to S.S.S. or A.J.L.

Competing financial interests

The authors declare no competing financial interests.

Methods

System information. We study a 10,000-particle Kob–Andersen model, a 80:20 binary LJ mixture¹⁶ with parameters: $\sigma_{AA}=1.0$, $\sigma_{AB}=0.8$, $\sigma_{BB}=0.88$, $\epsilon_{AA}=1.0$, $\epsilon_{AB}=1.5$, $\epsilon_{BB}=0.5$, $m_A=m_B=1$. Time is measured in units of $\tau=\sqrt{m_A\sigma_{AA}^2/\epsilon_{AA}}$ and the Boltzmann constant is $k_B=1$. We cut off the LJ potential at $2.5\sigma_{AA}$ and smooth the potential so that force varies continuously. This mixture has been characterized extensively. In particular, we compare our predictions to the measurements of the onset temperature in Keys and colleagues²⁰. Simulations were done using LAMMPS (ref. 22) in an NVT ensemble with a Nosé–Hoover thermostat and a time step of 0.0025τ . We output states every τ and quench them to their nearest inherent structure using a combination of conjugate gradient and FIRE algorithms. Throughout this study we use inherent structure positions. However, qualitatively similar results can be obtained using time-averaged positions. We study this system over the temperatures and number densities listed in Table 1.

Identifying rearrangements. We adapt a method first proposed by Candelier and colleagues^{23,24}. A timescale $t_R=10\tau$ is chosen to be commensurate with the amount of time the system takes to complete a rearrangement. Then two time intervals are defined as $A=[t-t_R/2, t]$ and $B=[t, t+t_R/2]$. An indicator function can then be written as

$$p_{\text{hop}}(t)=\sqrt{\langle(\mathbf{r}_i-\langle\mathbf{r}_i\rangle_A)^2\rangle_A\langle(\mathbf{r}_i-\langle\mathbf{r}_i\rangle_B)^2\rangle_B} \quad (1)$$

where $\langle\rangle_A$ and $\langle\rangle_B$ are averages over the intervals A and B respectively. p_{hop} is large when the mean position of a particle changes appreciably. Otherwise, it is similar in magnitude to the variance in particle positions due to noise from the inherent structure calculation.

To find rearrangements we restrict our attention to events in which p_{hop} exceeds a threshold of 0.05, which is large compared to the scale of fluctuations in particle positions but small compared to the typical value of p_{hop} during a rearrangement. As discussed in the Supplementary Methods, we define rearrangements to be those events with $p_{\text{hop}} > p_c = 0.2$. Changing this cutoff affects the results only quantitatively and manifests itself primarily as a shift in the energy scale, ΔE , which is approximately logarithmic in the cutoff. This agrees with the observations of Keys *et al.*²⁰, who saw a similar logarithmic shift in the energy scale governing rearrangements with the size of the rearrangements.

Note that rearrangements defined using p_{hop} result in particle displacements that follow a distribution that depends on the cutoff p_c used. This p_c dependence needs to be addressed when comparing the probability of rearrangement to the overlap function and its derivative, which are defined in terms of a length scale a . To do this, we multiply P_R by a temperature-independent constant c_a , namely the fraction of rearrangements that displace particles by more than a .

Computing softness. We have made two improvements that greatly increased the prediction accuracy for rearrangements compared to ref. 12. First, we identified rearrangements more carefully, as detailed above. Second, we defined our training sets more carefully. Each training set contains 6,000 particles that rearrange in the next time step, each labelled with $y_i=1$, as well as 6,000 particles that have not rearranged for a time τ_a before the structure was calculated, each labelled with $y_i=0$. These particles were chosen randomly from the set of all particles satisfying these conditions from MD simulations at a low temperature. Then, a training set of N particles can be written as $\{(\mathbf{F}_1, y_1), \dots, (\mathbf{F}_N, y_N)\}$, where $\mathbf{F}_i = \{F_i^1, \dots, F_i^M\}$ are the M structure functions that describe the local neighbourhood of particle i .

As in ref. 12 we use two classes of functions to generate the set of M structure functions. The first class measures the density of particles a distance $r \pm \delta$ from a reference particle, i ,

Table 1 | Number densities and temperatures studied.

ρ	1.15	1.20	1.25	1.30
T	0.37	0.45	0.58	0.70
	0.42	0.47	0.61	0.75
	0.45	0.51	0.69	0.84
	0.52	0.53	0.76	0.92
		0.56	0.97	1.12
		0.58		
		0.70		

Each column contains the temperatures studied for a given number density ρ .

$$G_X(i; r, \delta) = \sum_{j \in X} e^{-\frac{1}{2\delta^2}(r-R_{ij})^2} \quad (2)$$

where R_{ij} is the distance between particles i and j and X denotes a species whose density we wish to probe. By varying r , δ and X these functions investigate different aspects of the density of particles near the particle i . In this work we keep $\delta=0.1\sigma_{AA}$ fixed. The second class of functions counts the number of small (or large) bond angles between triples of particles within a distance ξ of one another. It is given by

$$\Psi_{XY}(i; \xi, \lambda, \zeta) = \sum_{j \in X} \sum_{k \in Y} e^{-(R_{ij}^2 + R_{jk}^2 + R_{ik}^2)/\xi^2} (1 + \lambda \cos \theta_{ijk})^\zeta \quad (3)$$

where θ_{ijk} is the angle between \mathbf{R}_{ij} and \mathbf{R}_{jk} , $\lambda=\pm 1$ determines whether we consider small or large bond angles, ζ determines the angular resolution, and X and Y are species. By varying X , Y , ζ , λ and ξ we probe different aspects of a particle's angular neighbourhood.

We then use an SVM to find the hyperplane $\mathbf{w} \cdot \mathbf{F} - b = 0$ that separates the points with $y_i=1$ from those with $y_i=0$. This hyperplane is used on the rest of the data to reach the results reported. The SVM is trained—that is, the hyperplane is constructed—on the binary variable y using the LIBSVM package¹⁴. It is not possible to find a hyperplane that perfectly separates the two different classes. We use a penalty parameter C and find the optimal hyperplane equation by minimizing

$$\frac{1}{2} \mathbf{w}^T \cdot \mathbf{w} + C \sum_{i=1}^N \chi_i \quad (4)$$

with the constraint $y_i \cdot (\mathbf{w}^T \cdot \mathbf{F}_i + b) \geq 1 - \chi_i$ and $\chi_i \geq 0$, where χ_i are the slack variables. The C parameter was chosen through cross-validation¹². The hyperplane obtained from this training can be used to classify a new particle neighbourhood, \mathbf{F}_n , as soft or hard. \mathbf{F}_n is soft if $\mathbf{w} \cdot \mathbf{F}_n - b > 0$, and hard otherwise. The continuous variable softness is defined by $S_n = \mathbf{w} \cdot \mathbf{F}_n - b$. See Supplementary Information for other classification schemes explored.

References

22. Plimpton, S. Fast parallel algorithms for short-range molecular dynamics. *J. Comput. Phys.* **117**, 1–19 (1995).
23. Candelier, R. *et al.* Spatiotemporal hierarchy of relaxation events, dynamical heterogeneities, and structural reorganization in a supercooled liquid. *Phys. Rev. Lett.* **105**, 135702 (2010).
24. Smessaert, A. & Rottler, J. Distribution of local relaxation events in an aging three-dimensional glass: temporal correlation and dynamical heterogeneity. *Phys. Rev. E* **88**, 022314 (2013).